Supplemental Method

Mouse primary LECs isolation

Mouse primary LECs were isolated from E14.5 embryonic skin. Tissue digestion was performed as described previously (Stanczuk et al, 2015). Briefly, embryonic skin was cut into smaller pieces for digestion using a mixture of 5 mg/ml Collagenase IV (Life Technologies) and 0.2 mg/ml DNase (Roche) in PBS with 5% fetal bovine serum (FBS) at 37°C under constant rotation for 45min. Digests were quenched by adding 2 mM EDTA and filtered through a 70-µm nylon filter (BD Biosciences). LECs were purified by using a MiniMACS separator and Starting Kit (Miltenyi Biotec). Briefly, digested cell solutions were centrifuged and resuspended in PBS with 0.5%BSA and 2 mM EDTA at approx 10^8 cells/ml. Macrophages and leukocytes were removed by adding rat anti-F480 and CD45 (BD Biosciences) antibodies and Goat anti-Rat IgG microbeads and purified on MACS MS column according to manufacturers' instructions. Flow through was collected and incubated with microbeads conjugated goat anti-Lyve1 antibodies. Lyve1 positive LECs were purified on MACS MS columns and eluted according to the manufacturers protocol.

Supplemental Reference

Stanczuk L., Martinez-Corral I., Ulvmar MH., Zhang Y., Laviña B., Fruttiger M., Adams RH., Saur D., Betsholtz C., Ortega S., et al. (2015). cKit Lineage Hemogenic Endothelium-Derived Cells Contribute to Mesenteric Lymphatic Vessels. *Cell Rep*. **10**,1708–1721.

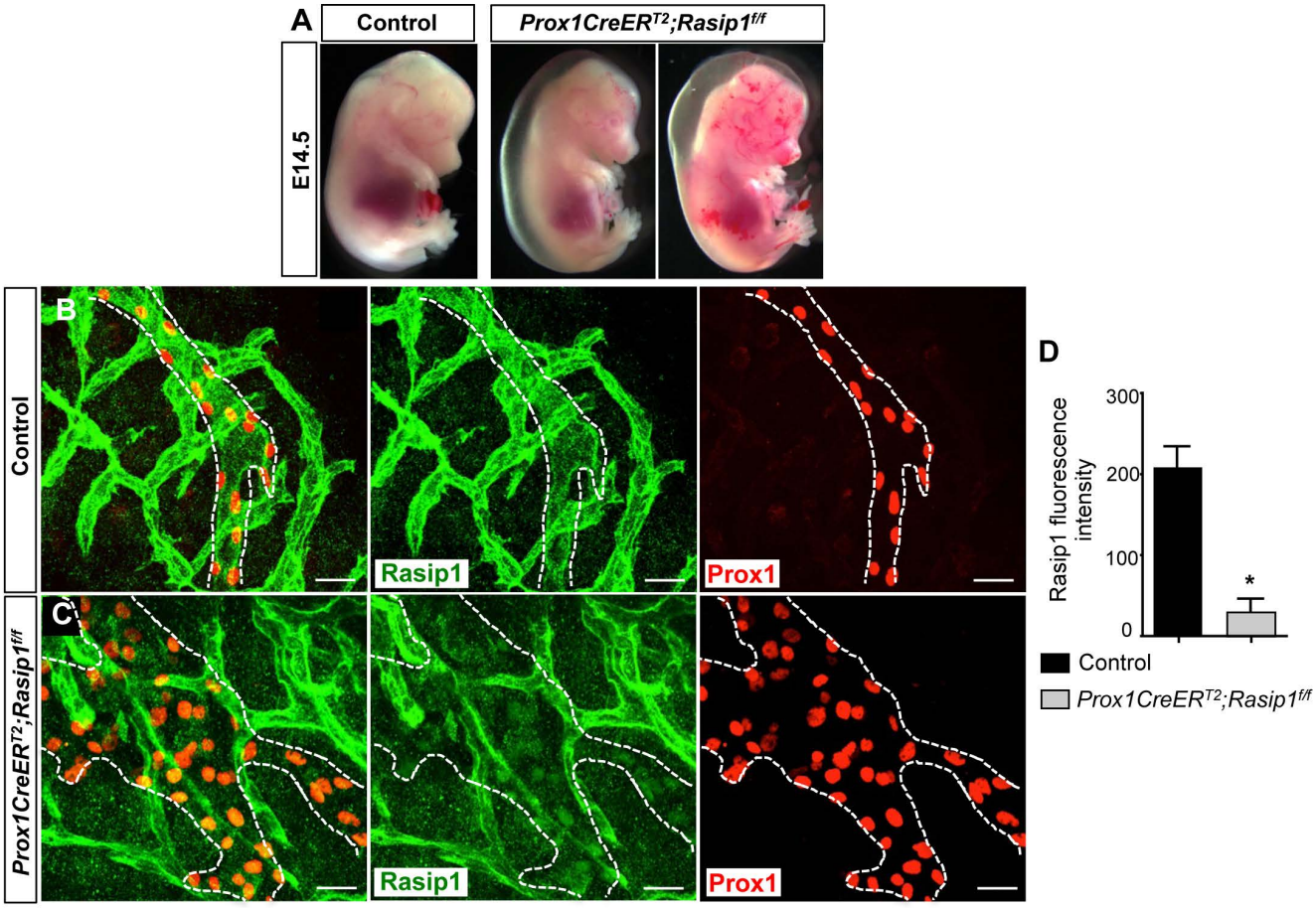

Fig. S1. Dermal lymphatics become enlarged and dilated in E14.5 *Prox1CreER^{T2};Rasip1$^{f/f}$* embryos

A) Representative images of E14.5 control and *Prox1CreER^{T2};Rasip1$^{f/f}$* embryos. *Prox1CreER^{T2};Rasip1$^{f/f}$* embryos exhibit severe edema (*n*=8) and some have also blood-filled lymphatics (*n*=4). **B, C)** Whole mount immunostaining of E14.5 dermal lymphatics of control (*n*=3) and *Prox1CreER^{T2};Rasip1$^{f/f}$* (*n*=3) embryos. Scale bar: 25 um. **D**) Quantification of Rasip1 fluorescence intensity in both genotypes. Data are derived from 6 fields per genotype. Results are expressed as mean ± SEM. **p*<0.05 vs control. Student T test.

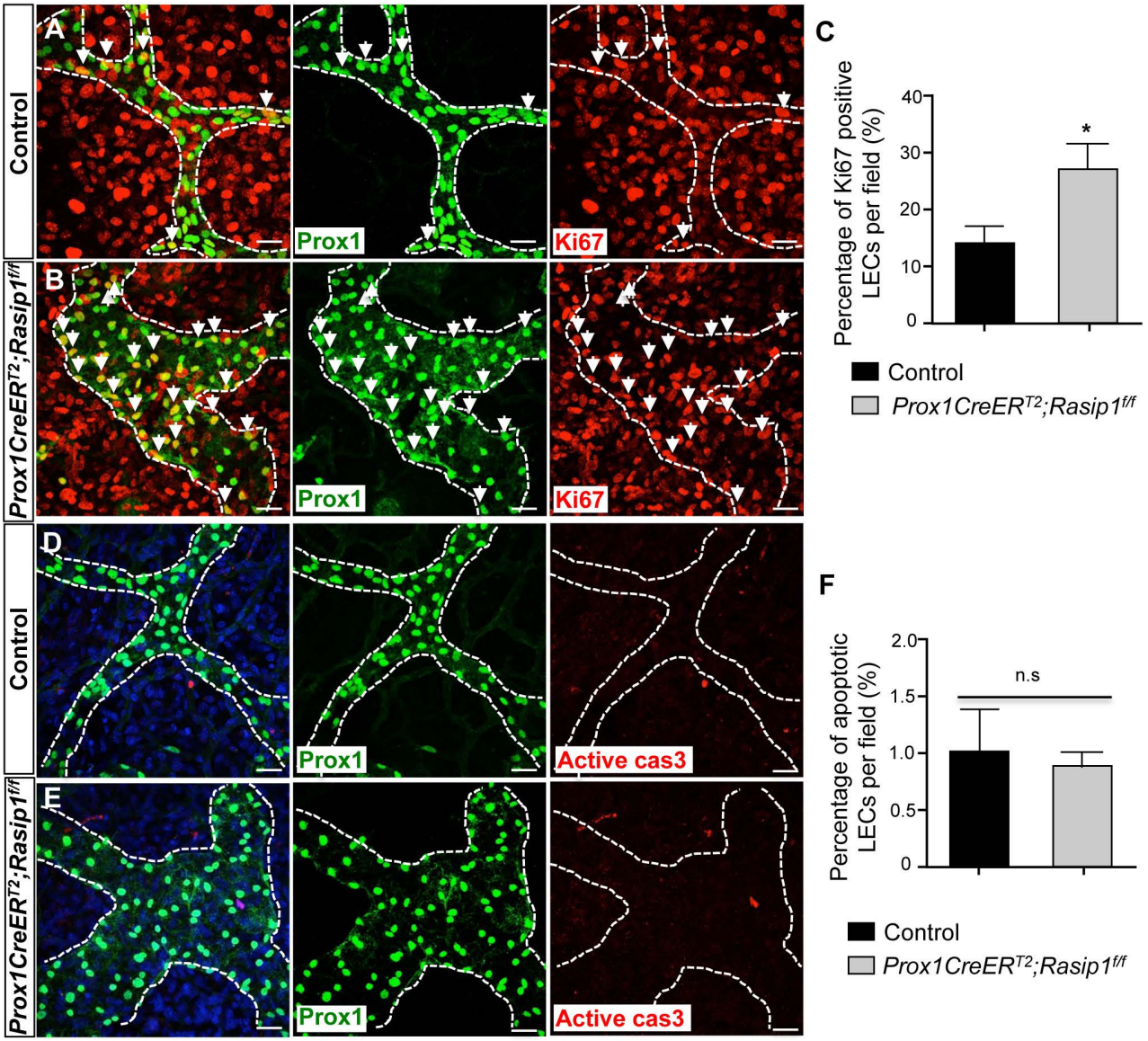

Fig. S2. Increased proliferation rate in skin lymphatics of E14.5 *Prox1CreER^{T2};Rasip1$^{f/f}$* embryos

A, B) Whole mount immunostaining of E14.5 skin lymphatics in control (*n*=3) and *Prox1CreER^{T2};Rasip1$^{f/f}$* embryos (*n*=3) using antibodies against Ki67 and Prox1. Arrows indicates Ki67 positive LECs. An obvious increase in the number of proliferating LECs is seen in the mutant embryos. Scale bar: 25 um. **C**) Quantification of the percentage of Ki67 positive LECs in both genotypes. Data are derived from 5 randomly selected fields per genotype. Results are expressed as mean ± SEM. **p*<0.05 vs control. Student T test. **D, E)** Whole mount staining of E14.5 skin lymphatics in control (*n*=4) and *Prox1CreER^{T2};Rasip1$^{f/f}$* embryos (*n*=3) with antibodies against active caspase-3 and Prox1. No obvious differences in cell death were observed. Scale bar: 25 um. **F)** Quantification of the percentage of active caspase-3 positive LECs in both genotypes. Data are derived from 5 randomly selected fields per genotype. Results are expressed as mean ± SEM. **p*<0.05 vs control. Student T test. TM was induced at E9.5 and E10.5.

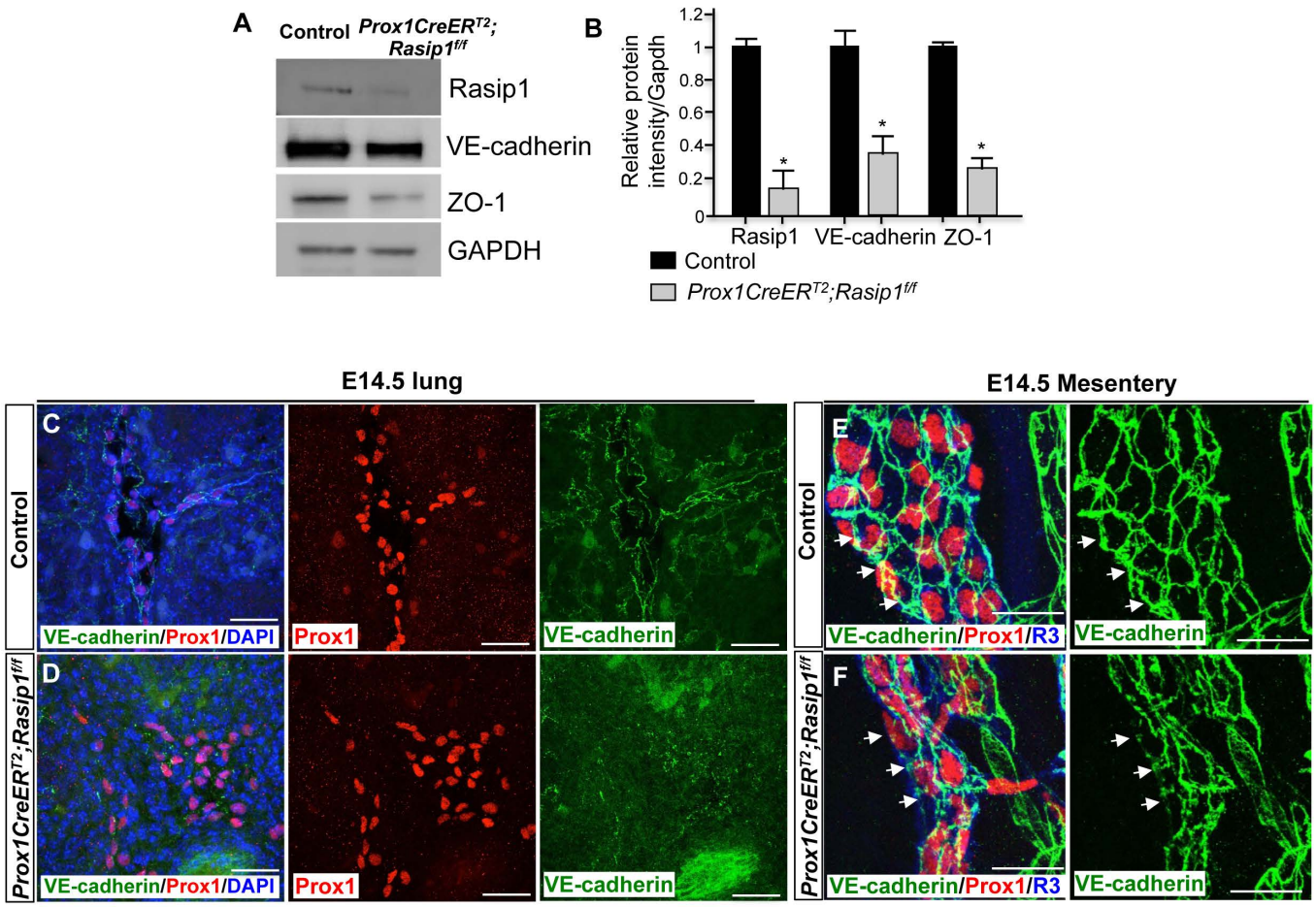

Fig. S3. Endothelial cell junctions are disorganized and expression of VE-cadherin is reduced in E14.5 *Prox1CreER^{T2};Rasip1$^{f/f}$* embryos

A) Western blot analysis of LECs isolated from E14.5 control (n=4) and *Prox1CreER^{T2};Rasip1$^{f/f}$* (n=4) skin lymphatics using antibodies against Rasip1, VE-cadherin, ZO-1 and GAPDH. As shown there, Rasip1 deletion was highly efficient and as seen *in vivo*, the levels of VE-cadherin and ZO-1 are reduced. **B)** Quantification of Rasip1, VE-cadherin and ZO-1 levels in isolated LECs of control and *Prox1CreER^{T2};Rasip1$^{f/f}$* embryos. Results are expressed as mean ± SEM of 3 triplicate experiments. **p*<0.05 vs control. Student T test. **C, D)** Immunostaining of thick sections (20 um) of lung lymphatics in E14.5 control (*n*=3) and *Prox1CreER^{T2};Rasip1$^{f/f}$* (*n*=3) embryos with antibodies against VE-cadherin and Prox1 and counterstained with DAPI. VE-cadherin-expressing junctions appeared disorganized in the mutant embryos. Scale bar: 50 um. **E, F)** Whole mount staining of E14.5 control (*n*=3) and *Prox1CreER^{T2};Rasip1$^{f/f}$* (*n*=3) mesentery lymphatics with antibodies against VE-cadherin, VEGFR3 and Prox1. Normal cell junctions are seen in control embryos (arrows); however, these are disorganized and diffuse in mutant embryos (arrows). Scale bar: 25 um.

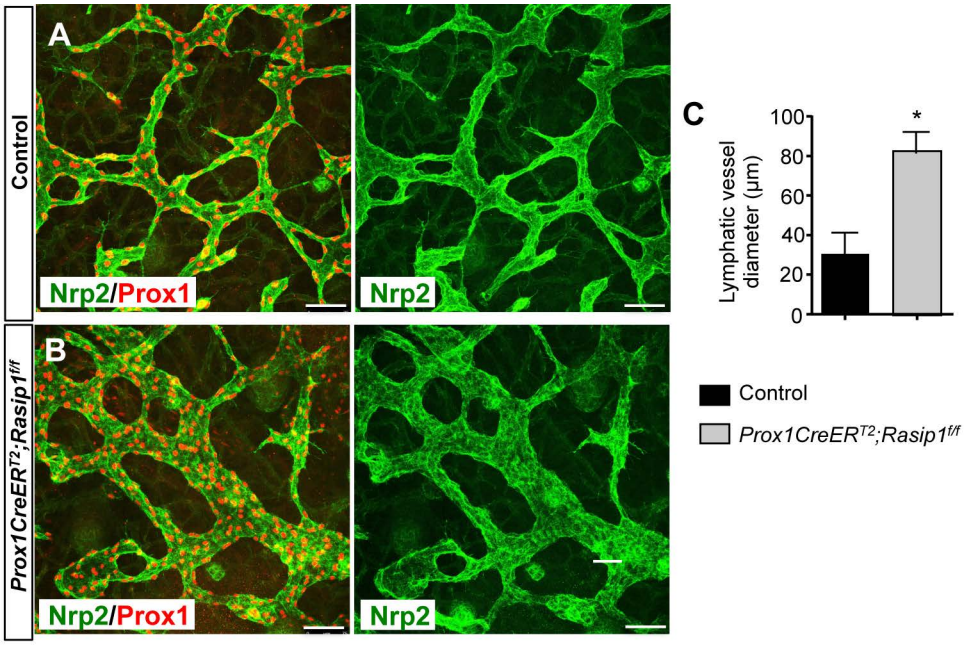

Fig. S4. Enlarged dermal lymphatic vessels in E14.5 *Prox1CreER^{T2};Rasip1$^{f/f}$* embryos

A, B) Whole mount staining of dermal lymphatics in E14.5 control (A) (*n*=3) and *Prox1CreER^{T2};Rasip1$^{f/f}$* (B) (*n*=3) embryos with antibodies against Nrp2 and Prox1. Scale bar: 75 um. **C)** Quantification of lumen diameters in dermal lymphatics of control and *Prox1CreER^{T2};Rasip1$^{f/f}$* embryos. Data are derived from 6 randomly selected fields per genotype. Results are expressed as mean ± SEM. **p*<0.05 vs control. Student T test. TM was induced at E9.5 and E10.5.

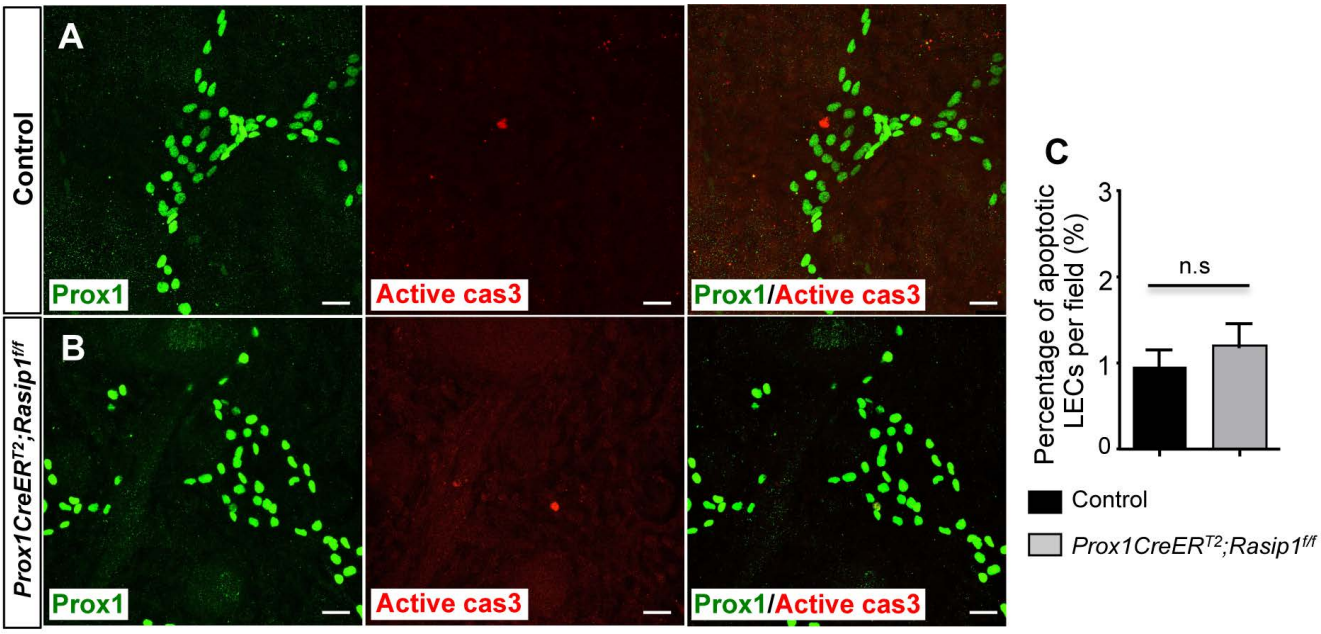

Fig. S5. No difference in LEC apoptosis in E16.0 *Prox1CreER^{T2};Rasip1$^{f/f}$* embryos

A, B) Whole mount staining of E16.0 control (*n*=3) and *Prox1CreER^{T2};Rasip1$^{f/f}$* (*n*=3) skin lymphatic vessels with antibodies against Prox1 and active caspase-3. Scale bar: 25 um. **C)** Quantification of percentage of active caspase-3 positive LECs in skin samples of E16.0 control and *Prox1CreER^{T2};Rasip1$^{f/f}$* embryos. Data are derived from 6 randomly selected fields per genotype. Results are expressed as mean ± SEM. Student T test. TM was induced at E9.5 and E10.5.

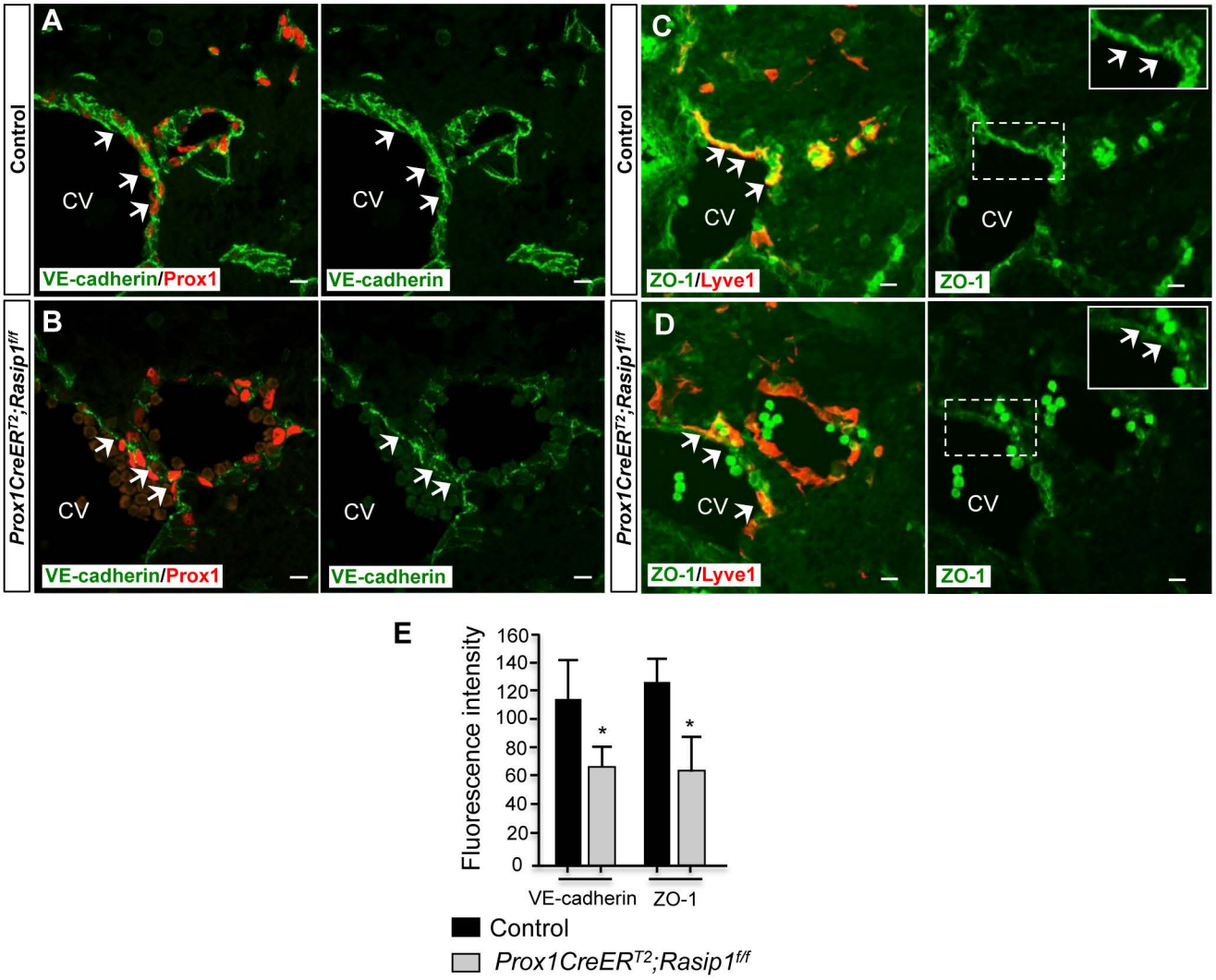

Fig. S6. LEC cell junction levels are reduced in E11.5 *Prox1CreER^{T2};Rasip1$^{f/f}$* embryos
A, B) Immunostaining of E11.5 transverse sections of control (*n*=3) and *Prox1CreER^{T2};Rasip1$^{f/f}$* embryos (*n*=3) at the level of the anterior cardinal vein (CV) with antibodies against VE-cadherin and Prox1. Arrows indicate Prox1-expressing LEC progenitors. LEC progenitors are seen also inside the CV of conditional mutant embryos and also budding off into the surrounding mesenchyme. However, the levels of VE-cadherin are strongly downregulated in those mutant LECs. **C, D)** Additional sections of E11.5 control (*n*=3) and *Prox1CreER^{T2};Rasip1$^{f/f}$* (*n*=3) embryos were immunostained against ZO-1 and Lyve1. Arrows indicate ZO-1 expressing LEC progenitors. Similar to VE-cadherin, the levels of ZO-1 were severely reduced in the mutant embryos. Upper right panels in green channels show higher magnification of selected regions. TM was induced at E9.5 and E10.5. Scale bars are all 10 um. **E)** Quantification of relative fluorescence intensity for VE-cadherin and ZO-1 staining at E11.5 in control and *Prox1CreER^{T2};Rasip1$^{f/f}$* embryos. Data are derived from 5 randomly selected fields per genotype per stage. Results are expressed as mean ± SEM. *p<0.05 vs control. Student T test.

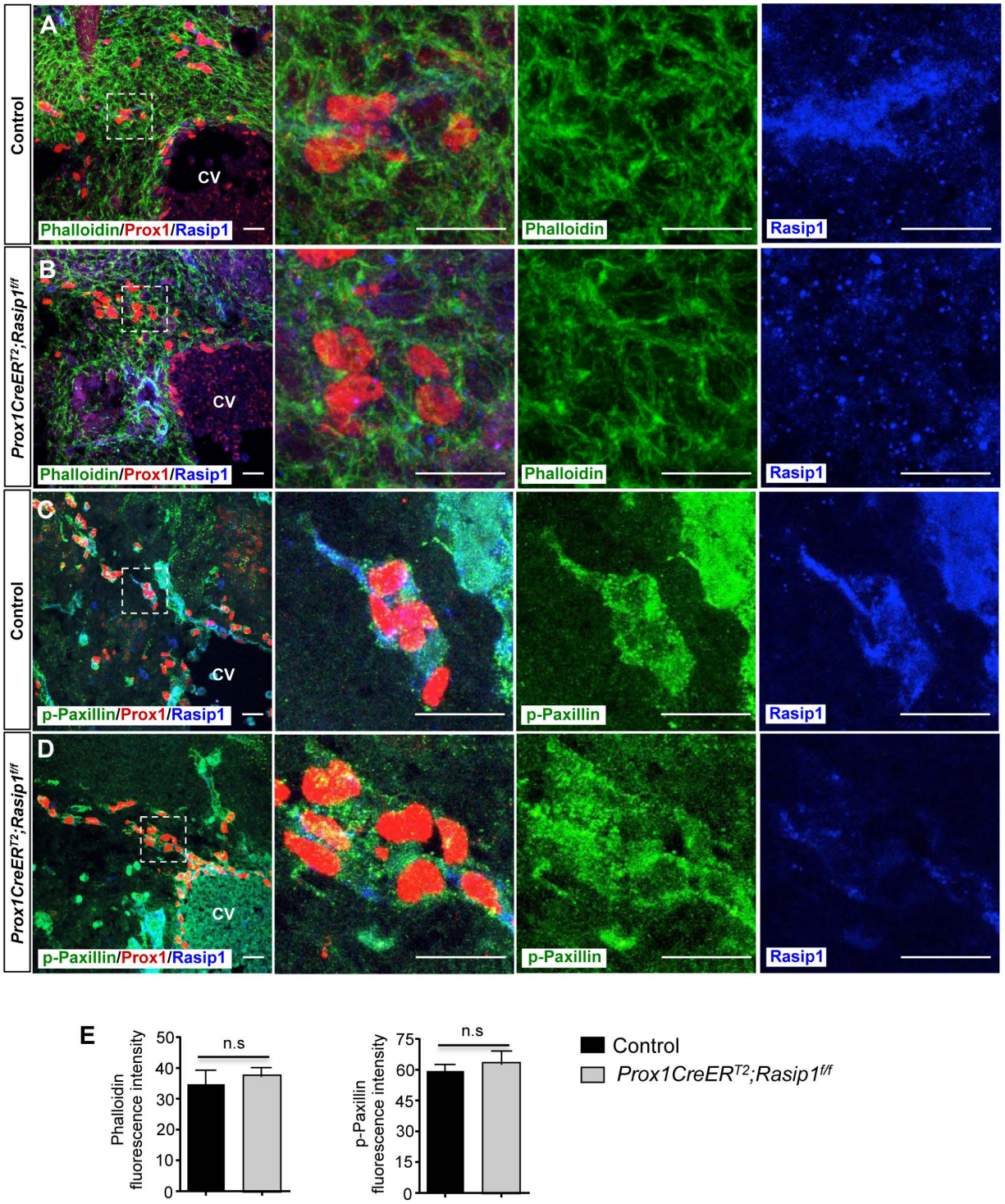

Fig. S7. No difference in cytoskeleton organization or LEC-ECM interactions in E11.5 *Prox1CreER^{T2};Rasip1$^{f/f}$* embryos

A-D) Immunostaining of E11.5 transverse sections of control (*n*=3) and *Prox1CreER^{T2};Rasip1$^{f/f}$* embryos (*n*=3) at the level of the anterior cardinal vein (CV) with 488-conjugated Phalloidin and antibodies against Prox1 and Rasip1 (A, B) or antibodies against p-Paxillin, Prox1 and Rasip1 (C, D). Right panels show higher magnification of selected regions. Rasip1 staining suggests sufficient deletion in LECs in *Prox1CreER^{T2};Rasip1$^{f/f}$* embryos. Scale bars are all 10 um. **E)** Quantification of fluorescence intensity for Phalloindin labeling and p-Paxillin staining in LECs in control and *Prox1CreER^{T2};Rasip1$^{f/f}$* embryos. Data are derived from 6 randomly selected fields per genotype per stage. Results are expressed as mean ± SEM. Student T test. TM was induced at E9.5 and E10.5.

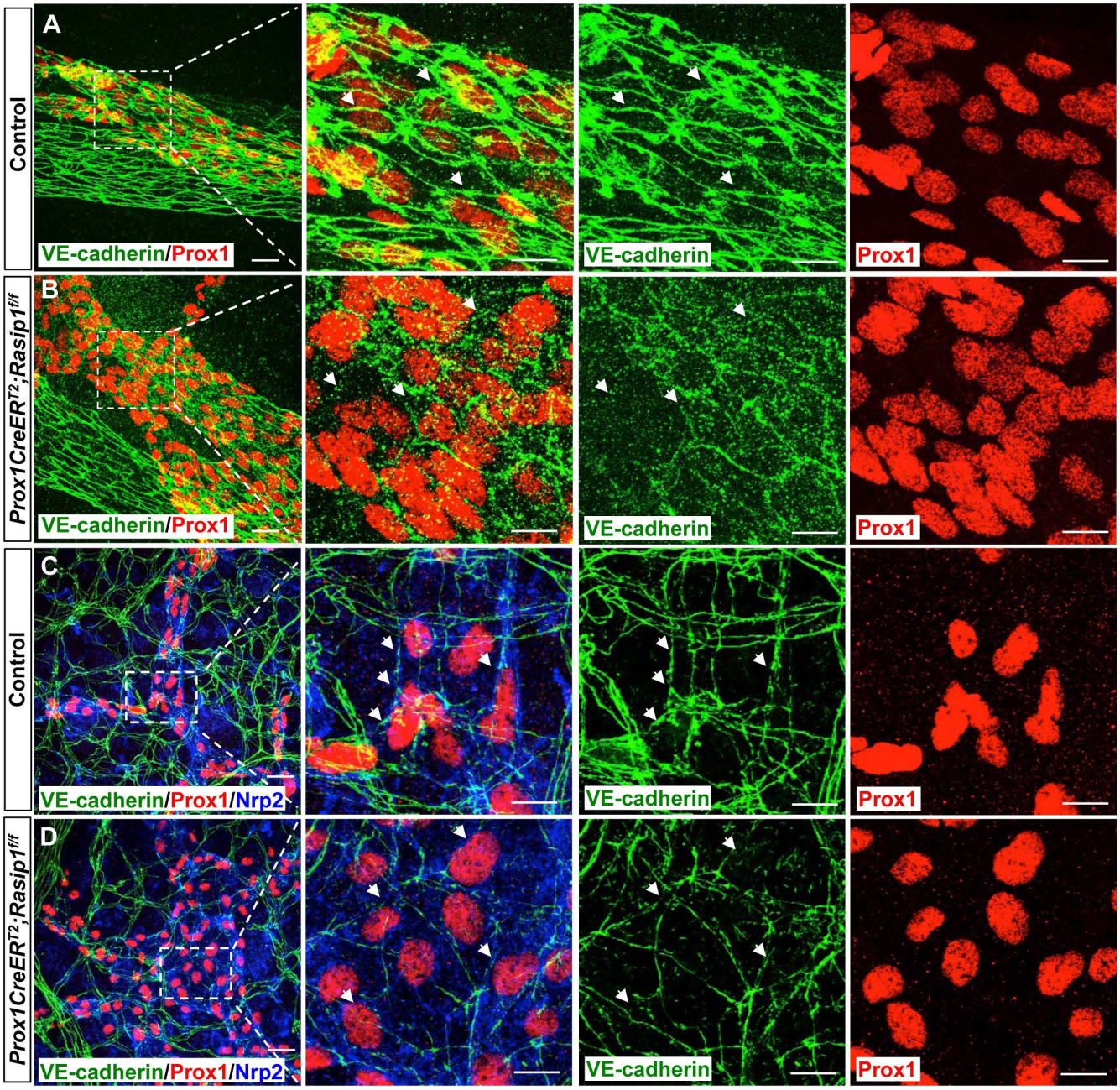

Fig. S8. Disorganized cell junctions in E17.5 *Prox1CreER^{T2};Rasip1$^{f/f}$* lymphatic vessels
A, B) Whole mount staining of mesentery lymphatics in E17.5 control (*n*=3) and *Prox1CreER^{T2};Rasip1$^{f/f}$* (*n*=3) embryos with antibodies against VE-cadherin and Prox1. The right panels show a higher magnification of the selected regions indicated in the left panels. White arrow indicates VE-cadherin junctions. Scale bar: 25 um. **C, D)** Whole mount staining of skin lymphatics in E17.5 control (*n*=3) and *Prox1CreER^{T2};Rasip1$^{f/f}$* (*n*=3) embryos with antibodies against VE-cadherin, Nrp2 and Prox1. The right panels show a higher magnification of the selected regions indicated in the left panels. White arrows indicate VE-cadherin junctions. TM was induced at E14.5. Scale bar: 25 um.

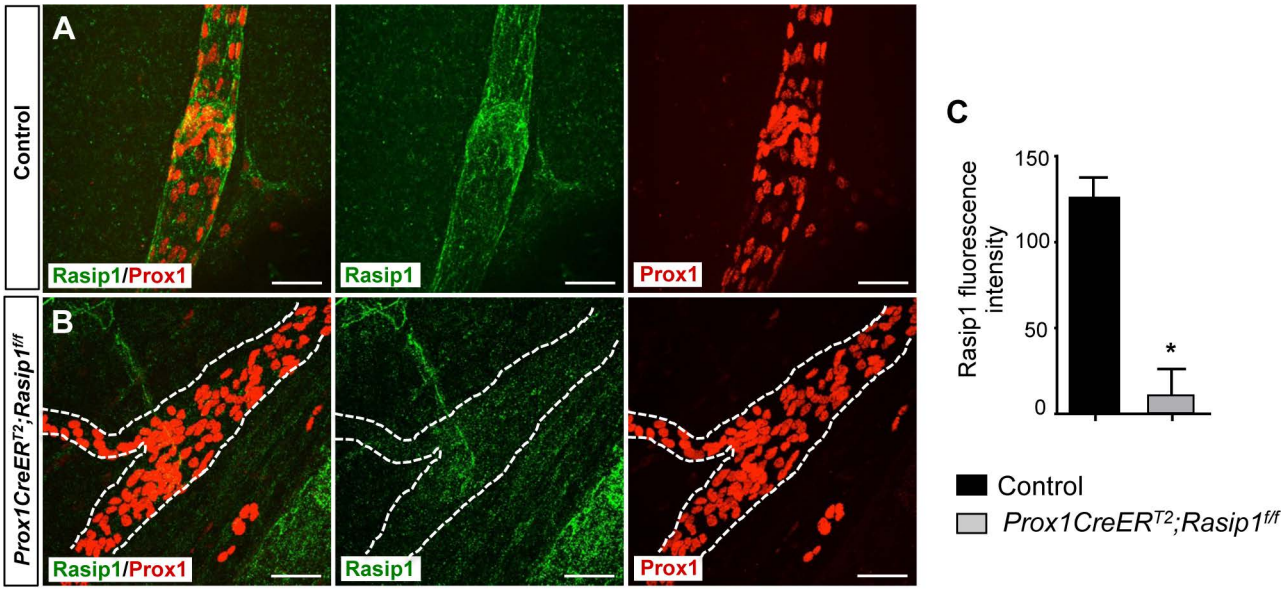

Fig. S9. *Rasip1* deletion efficiency in P6 *Prox1CreER^{T2};Rasip1$^{f/f}$* collecting lymphatic vessels

A, B) Whole mount staining of P6 mesentery lymphatics in control (*n*=5) and *Prox1CreER^{T2};Rasip1$^{f/f}$* (*n*=4) embryos with antibodies against Rasip1 and Prox1. Dashed line outline the collecting lymphatic vessel. Scale bar: 50 um. **C)** Quantification of fluorescence intensity for Rasip1 staining in control and *Prox1CreER^{T2};Rasip1$^{f/f}$* embryos. Data are derived from 6 randomly selected fields per genotype per stage. Results are expressed as mean ± SEM. **p*<0.05 vs control. Student T test. TM was induced from P0 to P4.

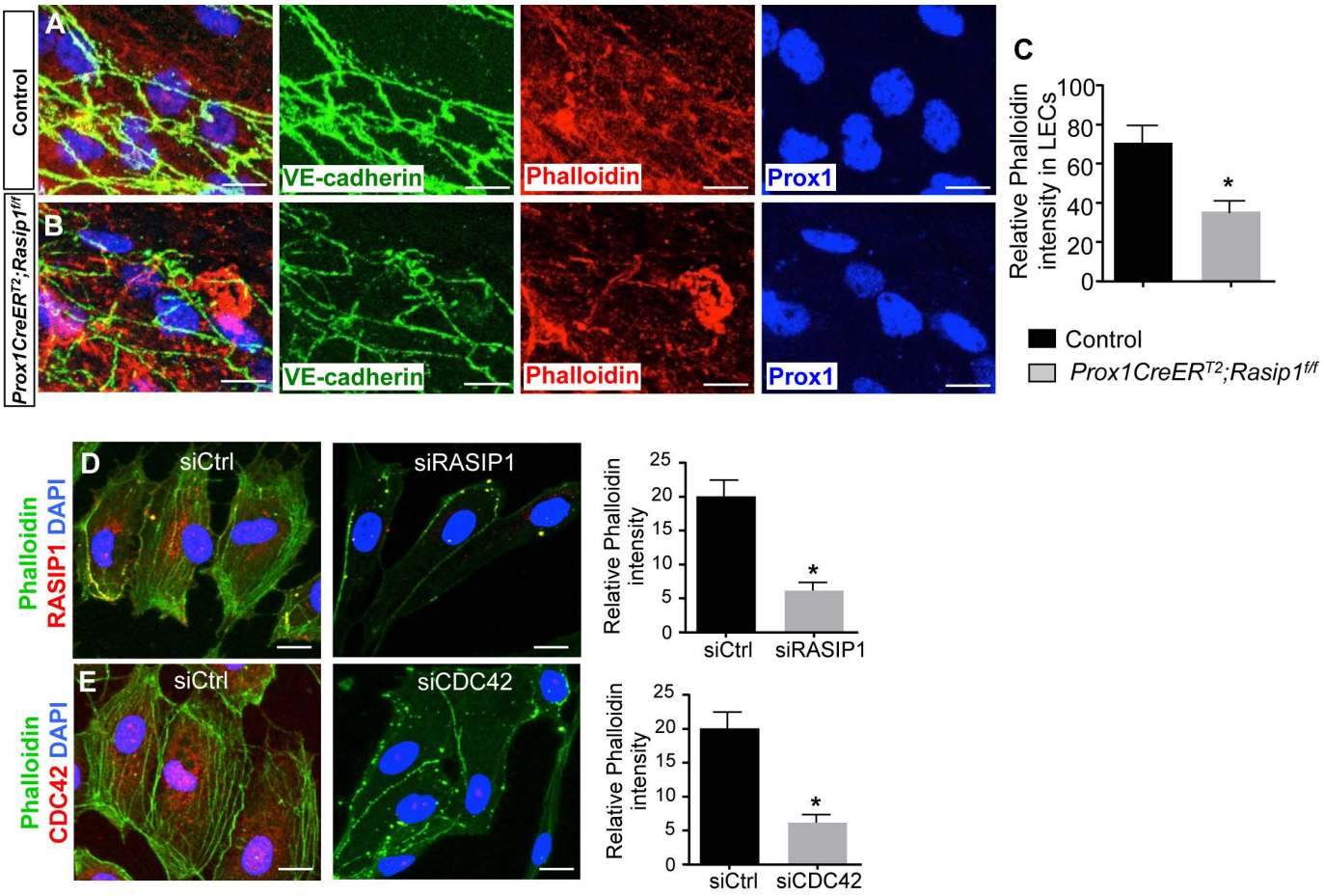

Fig. S10. Abnormal cytoskeleton organization in Rasip1 deficient LECs *in vivo* and *in vitro*
A, B) Whole mount staining of E14.5 mesentery lymphatics in control (*n*=3) and *Prox1CreER^{T2};Rasip1$^{f/f}$* (*n*=3) embryos with antibodies against VE-cadherin, Prox1 and Cy3-conjugated Phalloidin. TM was induced at E9.5 and E10.5. **C)** Quantification of Phalloidin intensity in mesentery lymphatics of control and *Prox1CreER^{T2};Rasip1$^{f/f}$* embryos. Data are derived from 5 randomly selected fields per genotype. Results are expressed as mean ± SEM. **p*<0.05 vs control. Student T test. **D, E)** Immunostaining of control, RASIP1 siRNA (siRASIP1) or CDC42 siRNA (siCDC42) treated human dermal LECs with antibodies against RASIP1, CDC42 and 488-conjugated Phalloidin. Experiments were repeated three times. Scale bars are all 10 um. Quantifications of Phalloidin intensity are shown at right panel. Data are derived from 5 randomly selected fields per genotype. Results are expressed as mean ± SEM. **p*<0.05 vs control. Student T test.

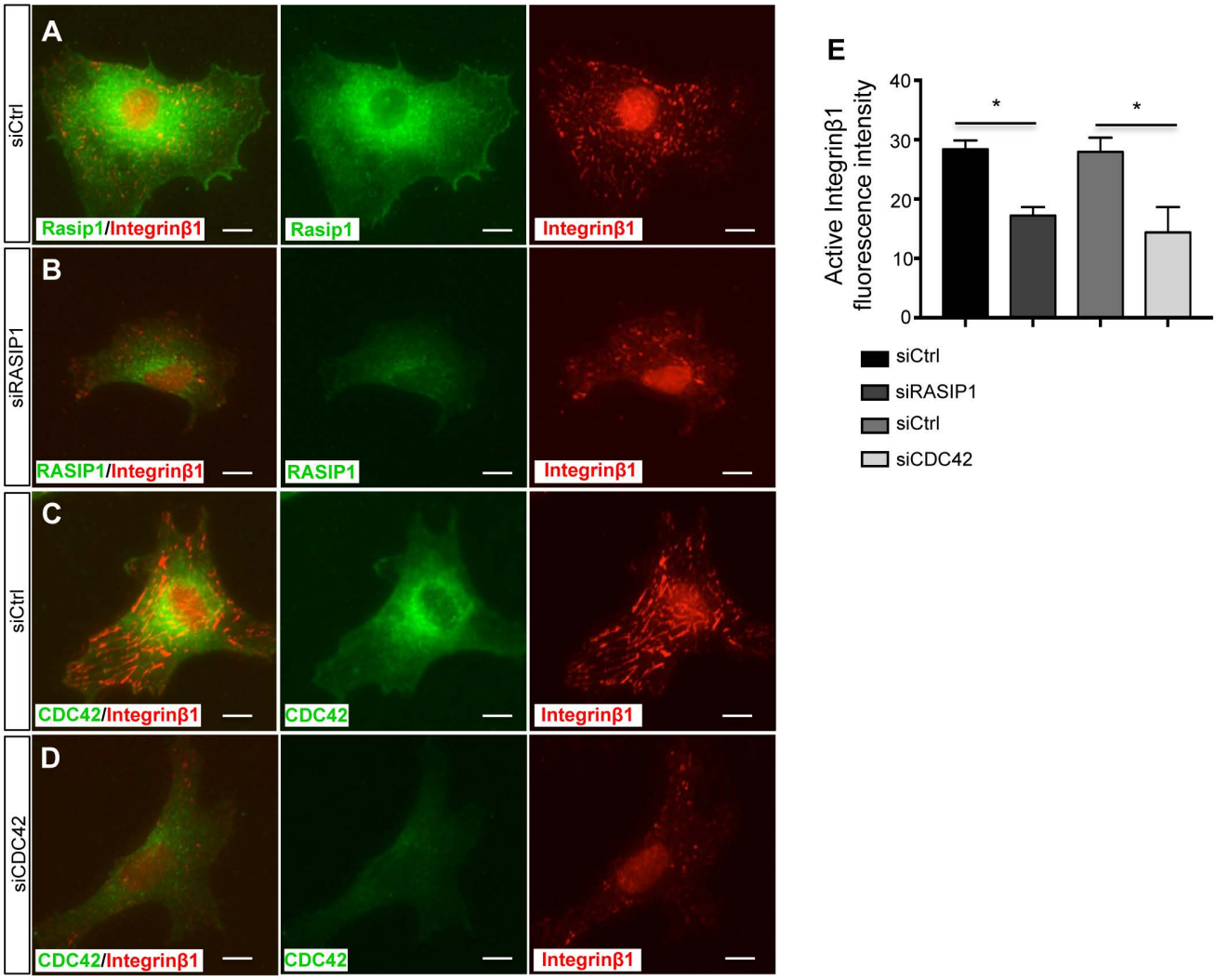

Fig. S11. Reduced mature focal adhesion activities in siRASIP1 or siCDC42 treated LECs. A-D) Immunostaining of siCtrl, siRASIP1 or siCDC42-treated LECs with antibodies against RASIP1 and active Integrinβ1 (A, B) or CDC42 and active Integrinβ1 (C, D). The levels of active Integrinβ1 are drastically reduced in the siRASIP1 or siCDC42-treated LECs. Scale bar, 10 um. **E)** Quantifications of active Integrinβ1 levels in siCtrl, siRASIP1 and siCDC42-treated cells. Data are derived from 6 randomly selected fields per group. Results are expressed as mean ± SEM. *p<0.05 vs siCtrl. Student T test.

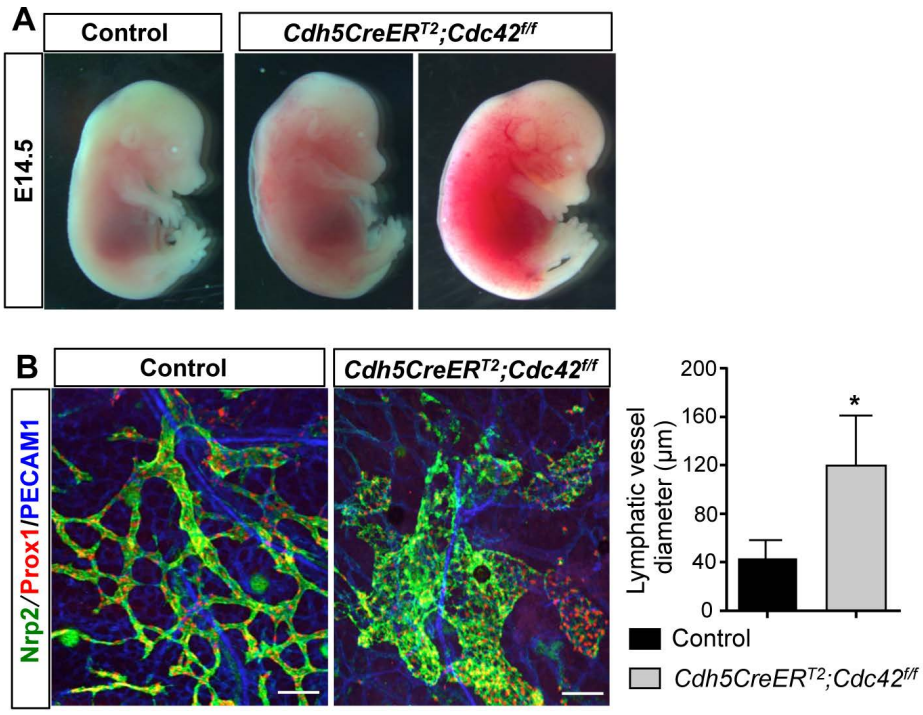

Fig. S12. Dermal lymphatics are enlarged and dilated in E14.5 *Cdh5CreER^{T2};Cdc42$^{f/f}$* embryos

A) Representative bright field images of E14.5 control (*n*=5) and *Cdh5CreER^{T2};Cdc42$^{f/f}$* (*n*=3) embryos. **B)** Whole mount staining of E14.5 dermal lymphatics of control (*n*=3) and *Cdh5CreER^{T2}; Cdc42$^{f/f}$* (*n*=3) embryos. Lymphatics are abnormally dilated in the mutant embryos. Scale bar: 100 um. Quantification of lymphatic vessel diameters in both genotypes is shown in the right panel. Data are derived from 6 randomly selected fields per genotype. Results are expressed as mean ± SEM. **p*<0.05 vs control. Student T test.

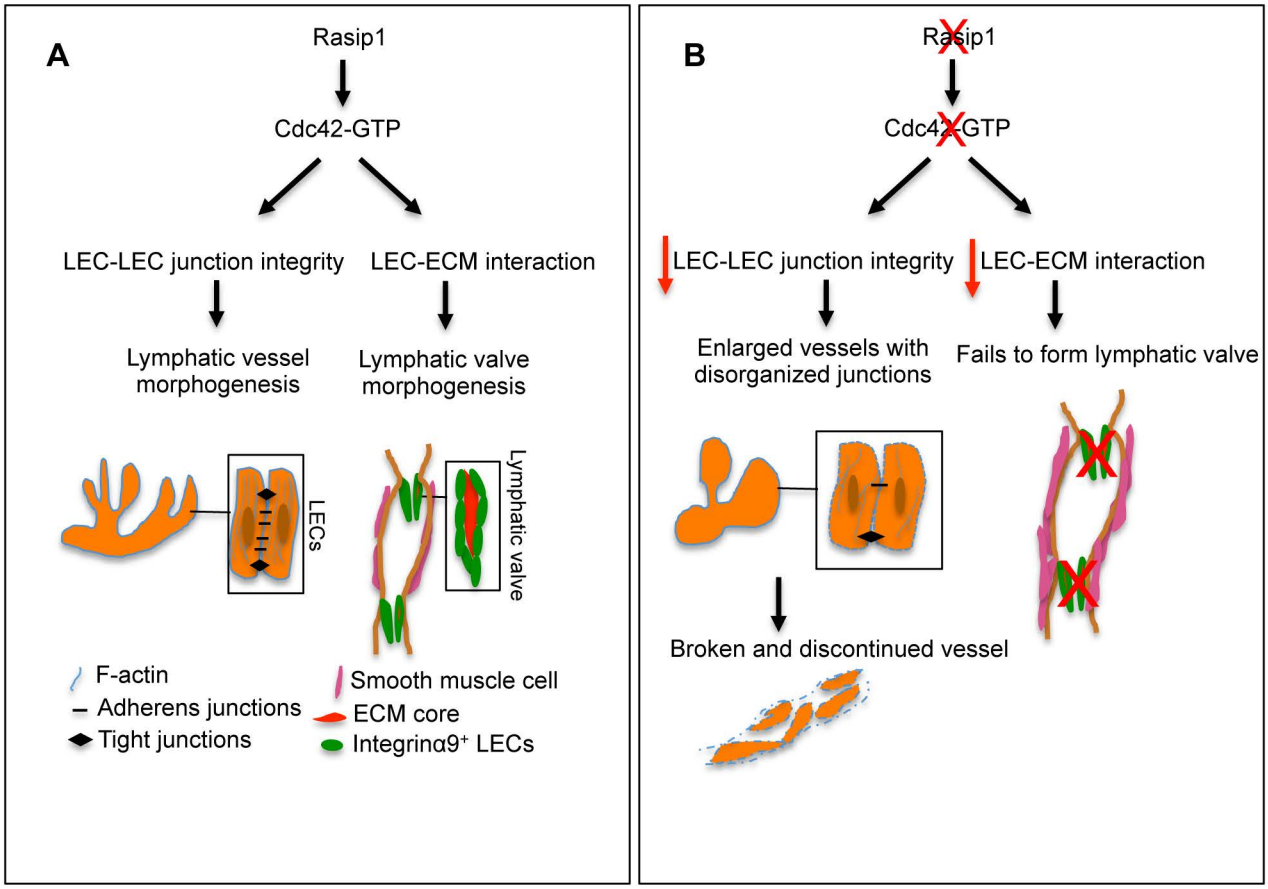

Fig. S13. *Rasip1* regulates LEC cell junction integrity and lymphatic valve formation by regulating Cdc42 activity

A) In control embryos *Rasip1* regulation of Cdc42 activity in LECs is required for cytoskeleton organization which in turn promotes lymphatic endothelial junctions' integrity to ensure lumen maintenance and proper lymphatic vessel morphogenesis. During lymphatic valve development, *Rasip1* regulates Cdc42 activity in valve-forming cells to modulate LEC interactions with the surrounding ECM. **B)** Loss of *Rasip1* abolishes Cdc42 activity, thus LECs show disorganized cytoskeleton localization which impairs proper LEC junctions' integrity. Therefore, developing lymphatic vessels get fragmented and lose their lumen. During lymphatic valve development, loss of *Rasip1* leads to defective LEC-ECM interactions in LECs resulting in defective lymphatic valve formation.